Geophys. J. R. astr. Soc. (1977) **50**, 441–458

A kinematic viscoelastic model of the San Francisco earthquake of 1906

John B. Rundle and David D. Jackson *Department of Geophysics and Space Physics, University of California, Los Angeles, California 90024, USA*

Received 1977 February 4; in original form 1976 September 1976

Summary. We construct a model of the San Andreas fault zone based on a rectangular fault in an elastic layer overlying a viscoelastic half-space. We alllow both steady and episodic aseismic slip at depth on the fault as well as a large-scale relative plate driving force. We use the model to explain the aseismic changes in geodetic triangulation angles observed during the 40 years following the 1906 San Francisco earthquake. The most important results are that viscoelastic relaxation can explain the data very well, and that the driving force of relative plate motion can be characterized by a horizontal distance scale perpendicular to the plate boundary of hundreds of kilometres.

1 Introduction

With the acquisition in recent years of geodetic triangulation and trilateration data along the San Andreas fault zone (Meade 1973) has come the realization that the data can perhaps illuminate some of the physical processes occurring along such a major strike slip fault. Observations of coseismic ground displacements have prompted the use of the elasticity theory of dislocations (Steketee 1958; Chinnery 1961, 1963; Maruyama 1964; Press 1965) to model an earthquake as the sudden appearance of a dislocation across a fault surface in an elastic medium. In addition, aseismic ground displacements observed at various locations along the San Andreas (Meade 1973) have been explained in a similar manner via stable sliding at depth along the fault. The fault slip is modelled by a steadily increasing dislocation across a slip surface in an elastic medium.

To date the most successful models of the San Andreas have been those of Savage & Burford (1973), Thatcher (1974, 1975a,b) and Turcotte & Spence (1974). Savage & Burford (1973) analysed the accumulation of tectonic strain in central California using models consisting of stable sliding along an infinitely long fault in a uniform elastic half-space. Thatcher (1974, 1975a,b) used finite and infinitely long dislocations in an elastic half-space to explain the pre-seismic, coseismic and post-seismic ground displacements associated with the San Francisco earthquake of 1906. Turcotte & Spence (1974) proposed that strain accumulation along the fault is due to stable slip at depth in the elastic lithosphere. They model the lithosphere by an elastic plate and thus assume that the asthenosphere is entirely decoupled from the lithosphere during the steady strain accumulation

process. Their model uses a constant shearing stress field to induce slip along an infinitely long, vertical surface of zero friction which begins at a depth D and extends to the bottom of the plate at a depth H.

Recent laboratory evidence (Brace & Byerlee 1966, 1970; Byerlee & Brace 1968) has suggested that rock may undergo a transition from dominantly brittle failure at shallow depths to aseismic slip at greater depths in the San Andreas fault zone. This may well explain why earthquakes on the San Andreas only occur at depths less than ~ 15 km (e.g. Brace & Byerlee 1970). In addition, Lachenbruch & Sass (1973) used heat-flow arguments to show that the San Andreas region can be represented by a model in which a brittle, seismogenic regime overlies a more ductile zone. Whether the ductility of their lower region is due to stress and temperature-dependent rock creep or whether it is due to another mechanism such as transient flow of ground-water is not known. However, creep may be an important element in the stress relaxation process if a relatively plastic material such as quartz (Hobbs, McLaren & Paterson 1972) is abundant below ~ 15 km.

None of the models of Savage & Burford (1973), Turcotte & Spence (1974) or Thatcher (1974, 1975a, b) completely include the effects of a transition to anelastic behaviour in all phases of the earthquake cycle. For example, although the model of Turcotte & Spence (1974) implicitly includes the long-term effects of a lower viscoelastic region, it does not include the transient effects. Rather, these models are intended to lend physical insight into complex phenomena and to explain in as clear-cut a manner as possible the origin of the geodetic observations collected over the years. We propose to go a step beyond the present models and represent the San Andreas region by an upper layer and a lower viscoelastic zone. We thereby hope to construct a quantitative model consistent with the work of Lachenbruch & Sass (1973). After constructing the model, we use it to explain the aseismic surface displacements observed following the San Francisco earthquake of 1906.

In previous papers (Rundle & Jackson 1977a and b) we outlined a means of calculating the surface displacements from a rectangular strike slip fracture in an elastic layer over a Maxwell viscoelastic half-space. We computed the ground displacements due to viscoelastic relaxation of the stresses caused by the introduction of a rectangular dislocation into the elastic layer.

We model the San Andreas fault as a surface fracture of depth D in the upper part of an elastic layer of thickness H overlying a Maxwell viscoelastic half-space. In the lower part of the elastic layer, between depths D and H, we permit the existence of both steady and episodic aseismic fault slip. We also assume that the driving mechanism causing strain accumulation along the fault gives rise to measurable surface displacements which can be represented simply. Thus in our model, aseismic ground displacement can occur through any combination of viscoelastic relaxation, steady fault slip, episodic fault slip and gross relative plate motion (Fig. 1).

We shall occasionally refer to the terms *lithosphere* or *plate* and *asthenosphere.* For our purposes, a mechanical definition of these terms will be adopted. The *lithosphere* or *plate* will be taken to be that topmost portion of the Earth that can support non-hydrostatic stresses for time periods of more than about 1 Myr. The stress of the lithosphere will be assumed to be linearly related to its strain, and its only allowed mode of failure will be brittle fracture. By contrast, we take the *asthenosphere* to be that portion of the Earth directly below the lithosphere which cannot support non-hydrostatic stresses for time periods longer than about 1 Myr. The stress of the asthenosphere will be taken to depend in some way upon both the strain and its time derivatives. Thus the asthenosphere can fail in a non-brittle way by 'flowing' to reduce its internal stresses.

The elastic layer of our model will be identified with the mechanically defined lithosphere and the viscoelastic half-space with the mechanically defined asthenosphere. If the elastic

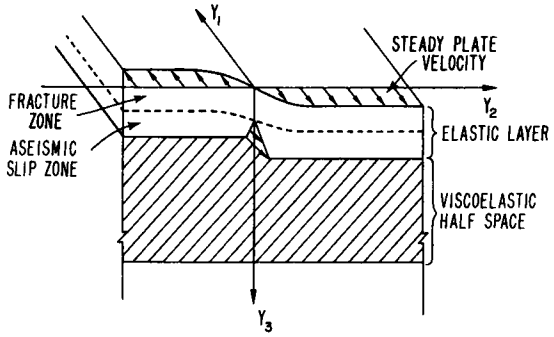

Figure 1. The San Andreas fault model.

layer thickness is less than ~ 20–30 km, the layer can also be identified with a crustal zone. Although the mechanical lithosphere is generally on the order of 50–200 km thick (Crittenden 1963; McConnell 1965) this identification does not diminish the importance of viscoelastic relaxation for the San Andreas area because the asthenosphere can conceivably extend to a shallow depth beneath a strike slip fault. The viscoelastic region A in Fig. 2 could result from shearing stresses in the vicinity of the fault which give rise to either a ductile material or to a medium saturated with water- or melt-filled cracks. Mavko & Nur (1975) have postulated a viscoelastic mechanism to explain the post-seismic adjustments following the Nankaido earthquake of 1946 based upon the opening and closing of cracks in the asthenosphere. They found that the applied forces can induce flow of a liquid melt contained within cracks thereby allowing viscoelastic relaxation with the correct time constant. In our case, transient flow of groundwater following Darcy's law could play a role similar to that of the melt in the Mavko & Nur (1975) model. Such a viscoelastic medium, together with a thin upper elastic layer, may comprise the Earth structure found at a major plate boundary such as the San Andreas. If this is true, the viscoelastic half-space would be the localized viscoelastic region A together with the larger region B in Fig. 2.

We note that other studies using different definitions of the lithosphere found widely varying values for its thickness. Leeds (1975) used surface wave dispersion to obtain oceanic lithospheric thicknesses in the western Pacific of 50 km for an age of 30 Myr increasing roughly linearly to 104 km for an age of 150 Myr. Crough (1975) used a thermal model to explain the increase of lithospheric thickness as due to cooling and thickening of the relatively thin lithosphere accreted at ocean rises. Isacks, Oliver & Sykes (1968) and Sclater & Francheteau (1970) both found ocean lithospheric thicknesses of 50–100 km and continental thicknesses of about 100–200 km. Jackson (1971a and b) found strong frequency-

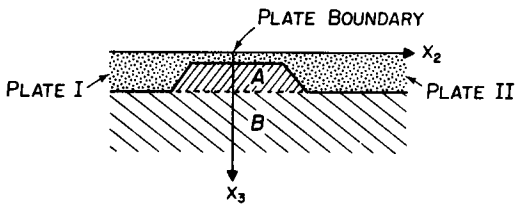

Figure 2. Possible variations in mechanical properties at a strike slip plate boundary. The lithosphere is dominantly elastic in regions far from the boundary of plates I and II while the asthenosphere, regions A and B, is viscoelastic in character and flows under applied forces. Near the plate boundary, the high shearing stresses combined with the presence of water or partial melt generated from shear heating transform the elastic properties of the plate in region A to those of a material which can flow viscoelastically under applied forces.

dependent regions of high Love wave and torsional oscillation attenuation extending from 50 to 400 km depth. If these high-attenuation regions can be identified with the asthenosphere, lithospheric thicknesses of hundreds of kilometres are implied.

2 Description of the model

The plate tectonic model of the Earth supplies a conceptual framework for the forces which drive the earthquake mechanism. An example of this is contained in the work of Forsyth & Uyeda (1975), who found that the balance of forces between gravity and buoyancy acting upon the slab at the trench boundary controls the motion of the rest of the plate. A second possible driving mechanism is convection. Here, the tractions driving the plates are applied at their bases. In both cases, it is physically reasonable to assume that the relative plate velocity between earthquakes is zero at the plate boundary and approaches a constant value far away.

Whichever driving force is dominant, its variation in the direction perpendicular to the plate boundary must be characterized by a horizontal distance scale y_0. Assuming that the plate boundary is locked through its entire thickness, the observed surface displacements resulting from the applied forces will also be characterized by the horizontal distance scale y_0. The most practical way to allow for the effects of the unknown forces upon the surface displacement profile of the model is to assume a simple, physically reasonable displacement function u_{DF}, involving both y_0 and the gross relative plate velocity $2V_0$. The data-fitting process should then yield information about the magnitudes of y_0 and V_0. We chose the function

$$u_{DF} = \frac{2V_0 R(t)}{\pi} \tan(y_2/y_0) \tag{1}$$

where V_0 is one-half the relative plate velocity far from the fault and $R(t)$ is the unit ramp function. As we are only interested in differences in displacement during a time interval Δt, $R(t)$ in equation (1) and following equations will be replaced by Δt when fitting the data.

Because the northern and southern portions of the San Andreas may not be locked throughout their entire thickness H, but only to some depth D, the displacement profile will be modified from equation (1) in a manner similar to that of Turcotte & Spence (1974). In their model the plate boundary was locked to a finite depth but freely sliding below that depth. The driving force was assumed to be a constant shear stress field, and the boundary conditions were zero stress upon both top and bottom of the plate and upon the stably sliding surface. They found that if D is approximately equal to H, the surface displacements increase linearly from the plate boundary in the neighbourhood of the boundary. When $D \ll H$ the surface displacements increase rapidly near the boundary but slow to the rate for the previous case at horizontal distances greater than about $2D$. Similarly we presume that in the absence of fault slip the driving forces induce the displacement profile given by equation (1). Thus if D/H is small, the observed plate velocity should increase more rapidly with distance normal to the fault than equation (1) and achieve a large value relatively near the plate boundary. On the other hand, if D/H is approximately unity, the displacement profile (1) should not be greatly modified.

Allowing the bottom portion of the plate to slip freely necessitates the introduction of a function describing the surface displacements due to the slip, which we assume to be steady in the lower portion of the plate and episodic in the middle. For the steady slip, we assume that the plates move by each other at their lower surfaces with relative velocity $2V_0$, thereby allowing the base of each plate at the boundary to 'keep up' with the motion on its upper

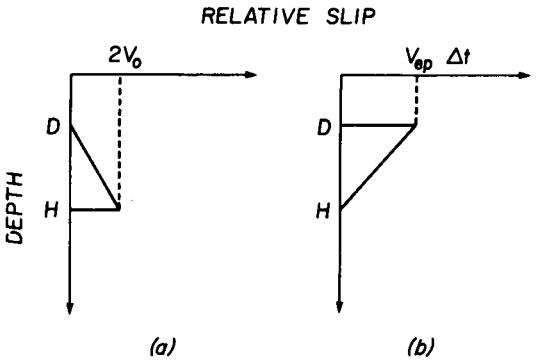

Figure 3. Diagram depicting the variation in relative aseismic slip at depth in the elastic layer for steady (a) and episodic (b) motion.

surface far from the boundary. We shall also assume that the steady state relative dislocation U_{ss} of the plates at the slip surface increases linearly downward from the depth D where they are pinned – see Fig. 3(a)

$$U_{ss} = 2V_0 R(t)\left(\frac{x_3 - D}{H - D}\right), \quad D < x_3 < H. \tag{2}$$

All transient effects associated with the onset of steady slip in the presence of the viscoelastic half-space will be neglected. To obtain the surface displacements due to the dislocation (2) which must be added to (1), we substitute (2) into the Green's function for a strike slip line source in an elastic layer over an elastic half-space and integrate over the slip surface (Rundle 1976; Rundle & Jackson 1977b).

The dislocation given in equation (2) should be thought of as an 'average', providing the physically reasonable result that little steady slip occurs at shallow depths in relation to larger depths. Note that equation (2) also has the effect of accumulating considerable stress between depths D and $\sim H/2$. The accumulated stress can be released by either a subsequent earthquake or by episodic slip. We shall ignore the former possibility because no moderate-to-large earthquakes were observed along the northern San Andreas at depths below 10 km during the 40 years following 1906, the time period we studied.

We chose the episodic dislocation function – see Fig. 3(b)

$$U_{ep} = V_{ep}\,[R(t - t_1) - R(t - t_2)]\,\frac{x_3 - H}{D - H} \tag{3}$$

where V_{ep} is a constant episodic slip velocity; $R(t)$ is the unit ramp function; $t_2 > t_1$; $H \geq x_3 \geq D$; t_1 and t_2 are respectively the beginning and ending times of the slip event.

Again, equation (3) should be thought of as representing an average dislocation which occurs mainly at intermediate depths in the plate below the zone of brittle fracture. The justification for using (3) together with (2) is the physically reasonable assumption that frictional strength on the fault decreases with depth. Thus a gradual transition from episodic slip at intermediate depths to steady slip at greater depths in the plate is expected.

The surface displacements due to episodic slip are obtained in the same manner as for steady slip except that the limit $t \to \infty$ is not taken.

Thus an important consequence of transient slip is that for times $t_1 < t < t_2$, ground displacements increase in magnitude at an accelerating rate. When slip begins, the viscoelastic half-space becomes stressed and relaxation also begins. Thus as time progresses, the ground

motion at a point is the sum of displacement due to both slip in an elastic half-space and to an ever-increasing amount of viscoelastic relaxation.

While steady slip and gross plate motion both move plate mass steadily throughout geologic time, brittle fracture and episodic slip proceed spasmodically. To conserve mass the relation

$$\frac{1}{D}\left\langle \int_0^D u_f \, dx_3 \right\rangle = \frac{1}{H-D}\left[\left\langle \int_D^H u_{ep} \, dx_3 \right\rangle + \int_D^H u_{ss} \, dx_3 \right] = 2V_0 \Delta t \tag{4}$$

must hold, where:

(i) u_f is the relative displacement across the plate boundary for $D \geqslant x_3 \geqslant 0$ due to brittle fracture;

(ii) u_{ep} is the relative displacement across the plate boundary for $H \geqslant x_3 \geqslant D$ due to episodic slip;

(iii) u_{ss} is the relative displacement across the plate boundary for $H \geqslant x_3 \geqslant D$ due to steady state slip; and where $\langle\rangle$ denotes an average over geologic time.

In the data inversion, we do not impose constraint (4) because we do not believe that the time period spanned by the observations, less than one century, qualifies as 'geologic time'.

Assuming that constraint (4) is fulfilled, the sum of the displacements produced by (1), (2) and (3) should have essentially the same time-averaged properties as does the Turcotte–Spence model. When $D \approx H$, expressions (2) and (3) are only small perturbations on (1). When D/H is small the surface displacements increase more rapidly than equation (1) close to the plate boundary but approach the constant value $V_0 \Delta t$ given by (1) far away.

In summary, our explanation of the surface displacements observed after the 1906 San Francisco earthquake incorporates the following mechanisms:

(i) Prior to 1906, gross plate motion and steady slip along the unlocked portion of the plate boundary stressed the fault zone;

(ii) The earthquake of 1906 ruptured the plate boundary to a depth D;

(iii) The upper portion of the boundary became re-locked and transient relaxation of the viscoelastic region, steady state slip and steady state plate motion succeeded the fracture event. These latter motions have continued to accumulate stress on the upper part of the plate boundary with the result that another earthquake will eventually occur.

3 Assumptions in the model

In our model we use the fault parameters for the 1906 earthquake as determined by Thatcher (1975a). The depth of faulting is taken as a uniform 10 km, and the dislocation function consists of six connected constant dislocations from San Juan Bautista in the south to Point Arena in the north.

We also assume that the elastic layer is flat, homogeneous and isotropic, and that there is no structure or surface topography. Although the validity of this assumption is open to question, any spurious displacements due to these effects can be treated as 'noise' in the observations. Since there is no reason to believe that any station is inordinately affected, effects incompatible with the model are minimized. Thus the assumed data error, 2 arcsec, includes not only observational error but also the errors produced by our simplifying assumptions.

We also assume that the viscous properties of the half-space are Newtonian. As it is not our purpose here to enter the debate upon the rheological properties of the Earth, we simply remark that a realistic earth model demands the inclusion of elastic as well as viscous

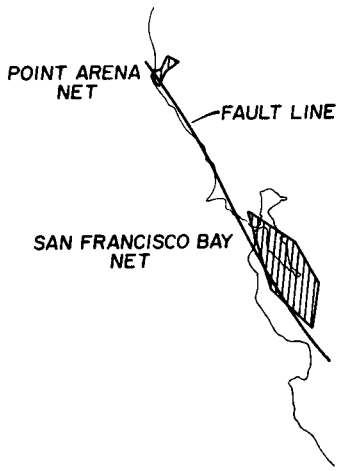

Figure 4. Map of the triangulation nets used. See Meade (1973).

properties in the stress-relaxing region (Peltier 1974; Rundle 1976). Using linear viscoelasticity by way of the correspondence principle is the most practical way to achieve this.

The final assumption is that neither the Hayward nor the Calaveras fault significantly participated in the shear straining along the San Andreas fault for the 30–40 years following the 1906 earthquake. Thatcher (1974b) found that the direction of maximum shear straining remained roughly parallel to the San Andreas until 1940, when it began to align more with the Calaveras fault. We therefore feel that our assumption is partially justified.

The triangulation data are described in detail in Meade (1973), Thatcher (1974, 1975a, b) and Rundle (1976). We used 28 angle changes spanning the years 1907–1947 from the San Francisco Bay area and 40 from Point Arena over the years 1907–1930 (Fig. 4). The reason for this relatively small number of data is that not all triangulation monuments were observed in successive surveys. Also, some were not observed immediately following the earthquake of 1906, so that the amount of displacement due directly to the earthquake is not known. Finally, one station, at Point Arena Lighthouse, was evidently moved in 1906 an unrecorded amount.

In order to use these data to fix the values of the model parameters, we used the inversion techniques developed by Jackson (1972, 1973, 1974). In this method, partial derivatives of the ground displacements predicted by the model are taken with respect to the model unknowns. These partial derivatives are used to form a square matrix which can be decomposed into its eigenvectors and eigenvalues. The eigenvalues and eigenvectors are used in an iterative way to construct the model best fitting the data and to give information on the accuracy to which the model parameters can be known.

We first picked a starting model and then used an iterative process to arrive at a final model. For example, 50 and 20 km were chosen as the starting values of elastic layer thickness H. $H = 50$ km was picked because it is roughly the minimum thought to be appropriate for a mechanical continental lithosphere; for larger H, viscoelastic relaxation plays little role in the surface displacements since the depth of faulting is small compared to H.

A Maxwell relaxation time τ of 5 yr was used because other authors have found viscoelastic relaxation times of this magnitude in similar studies of crustal rebound induced by thrust faulting (Nur & Mavko 1974). Note that τ is defined as η/μ_0, where η is the half-space effective viscosity and μ_0 is the rigidity of both elastic layer and half-space. Several one-parameter inversions were done using $\tau = 5$ yr whose purpose was to bound the thickness of

the elastic layer assuming the Mavko & Nur (1975) viscoelastic relaxation mechanism is valid. Other values of τ were also tested to see whether models with higher viscosities could fit the data.

The parameter y_0, which reflects the scale for the plate driving forces, has an unknown magnitude and so it was allowed to vary from 20 to 300 in the inversions. Small y_0 presupposes a driving force system resembling a step function across the boundary and produces a correspondingly sharp surface velocity profile. By allowing y_0 to vary, a wide variety of plate motions can be represented. The parameter V_0 is expected to be of the order of a few cm/yr on the basis of other work (Savage & Burford 1973; Minster *et al.* 1974). As noted above, V_0 is one-half the gross relative motion between the Pacific and North American plates, and in the coordinate system we use, right lateral motion is negative.

We have also chosen to analyse the data primarily with models which do not allow episodic aseismic slip. Previous work (Thatcher 1974, 1975a, b) has shown that the data can be explained by episodic slip alone. Hence we shall concentrate mainly on models without episodic slip and later show that the full model with all possible displacement mechanisms can also explain the data.

Table 1. Results of the inversions. H is the elastic layer thickness, τ is the characteristic stress relaxation time for the half-space, y_0 is the horizontal distance scale for the plate driving force and $2V_0$ is the gross relative plate velocity. Right lateral motion corresponds to negative V_0. Episodic aseismic slip is not allowed in these models.

Model No.	H (km)	τ (yr)	y_0 (km)	V_0 (cm/yr)	Aseismic slip	Inversion parameters
San Francisco Bay Area						
1	20.0	5.0	20.0	−1.0	No	H, τ, y_0, V_0
2	20.0	5.0	20.0	−1.0	Yes	H, τ, y_0; V_0 fixed
3	20.0	20.0	20.0	−1.0	Yes	H, τ, y_0, V_0
4	20.0	1000.0	20.0	−1.0	Yes	H, τ, y_0, V_0
5	20.0	10.0	50.0	−1.0	Yes	H, τ, y_0, V_0
6	50.0	5.0	50.0	−1.0	No	H, τ, y_0, V_0
7	50.0	20.0	5.0	−1.0	Yes	H, τ, y_0; V_0 fixed
8	50.0	1000.0	20.0	−1.0	Yes	H, τ, y_0, V_0
9	50.0	1000.0	20.0	−1.0	No	H, τ, y_0, V_0
10	50.0	1000.0	50.0	−1.0	No	H, τ, y_0, V_0
11	10.1	993.3	250.0	−2.75	No	H, τ, y_0, V_0
12	10.1	993.3	35.0	−2.75	No	y_0; H, τ, V_0 fixed
13	20.0	5.0	150.0	−2.75	No	H, τ, y_0, V_0
14	10.5	5.0	250.0	0	No	H, τ, y_0, V_0 fixed
Point Arena						
1	31.6	3.8	52.3	−1.08	Yes	H, τ, y_0, V_0
2	20.5	5.0	21.0	−0.13	No	H, τ, y_0, V_0
3	20.2	5.1	21.0	−0.08	No	H, τ, y_0, V_0
4	27.2	20.1	27.5	−0.88	Yes	H, τ, y_0, V_0
5	20.0	1000.0	20.5	−0.58	No	H, τ, y_0, V_0
6	32.1	1000.0	27.9	−0.67	Yes	H, τ, y_0, V_0
7	50.0	5.0	50.0	−1.15	Yes	H, τ, y_0, V_0
8	50.0	5.0	50.0	−1.26	No	H, τ, y_0, V_0
9	50.0	20.0	50.0	−1.32	No	H, τ, y_0, V_0
10	50.0	1000.0	50.0	−1.27	Yes	H, τ, y_0, V_0
11	10.1	997.7	263.6	−2.75	No	H, τ, y_0; V_0 fixed
12	50.0	1000.0	70.0	−2.75	No	H, τ, y_0; V_0 fixed
13	17.0	5.0	250.0	0	No	$H; \tau, y_0, V_0$ fixed
14	15.0	1000.0	80.0	−2.75	No	y_0; H, τ, V_0 fixed

4 Results

4.1 MODELS WITHOUT EPISODIC SLIP

In Table 1 we show the wide variety of models we found that fit the data. Clearly, models allowing viscoelastic adjustment are strong candidates for explaining the post-seismic angle changes. The assumption that aseismic slip in an elastic half-space is the only physically reasonable mechanism that can explain the data is not justified. Many combinations of aseismic slip, viscoelastic relaxation, and steady plate motion can explain the observations well.

Because of the large number of acceptable models, a statement of each model's parameters together with standard deviations gives a rather confusing picture. The technique that we chose to analyse the results is to pose the following series of questions; the answers should give an illustration of the kinds of physically admissible models:

(1) For given values of H, τ, y_0, v_0:

(i) Can a model which allows aseismic slip and a steady plate velocity fit the data?

(ii) Can a model which allows viscoelastic relaxation and a steady plate motion fit the data?

(iii) Can a model which allows aseismic slip, viscoelastic relaxation and a steady plate motion fit the data?

(iv) Can a model with viscoelastic relaxation alone fit the data?

(2) For a given y_0 and V_0, can a model which allows only steady plate motion explain the data?

(3) Can a model with V_0 set equal to the value found by Minster *et al.* (1974) from plate rotation pole studies fit the data?

(4) Can bounds be put on the parameters?

We start by considering the inversions of the Bay area data. Using Table 1, the following models with 'thick' elastic layers can be said to fit the data to within one standard deviation:

(i) Aseismic slip and steady plate motion;
(ii) Viscoelasticity in the lower half-space and steady plate motion;
(iii) Aseismic slip, viscoelasticity and steady plate motion.

Similarly, models with a 'thin' elastic layer and with the following characteristics also fit the data to within one standard deviation:

(i) Aseismic slip and steady state plate motion;
(ii) Viscoelasticity and steady state plate motion;
(iii) Aseismic slip, viscoelasticity, and steady state plate motion;
(iv) Viscoelasticity alone.

Finally, steady state plate motion alone was able to explain the observations, answering question (2) affirmatively.

Turning to question (3), let us set $V_0 = -W_0/2$, where W_0, the relative right lateral plate motion in northern California, has the value 5.5 ± 1 cm/yr found by Minster *et al.* (1974). Models 11B, 12B, 13B, (the B denotes Bay area models) with $V_0 = -2.75$ cm/yr, do fit the data well. Thus if the relative right lateral plate motion W_0 is 5.5 cm/yr, the distance scale y_0 can be large.

Examination of the geodetic data by other investigators, however, has produced relative right lateral displacements across the San Andreas of less than 5.5 cm/yr, implying a smaller

lower bound on y_0. Thatcher (1975b) found relative right lateral displacements of 5.8 ± 1.0 cm/yr across the Hayward triangulation net in a direction parallel to the Calaveras fault, and a value of 2.6 ± 0.8 cm/yr across the Point Reyes–Petaluma net parallel to the San Andreas. Savage & Burford (1973) found 3.2 ± 0.5 cm/yr of relative displacement in central California. These estimates were derived in a model-independent way from measurements taken within a few tens of kilometres of the trace of the San Andreas. In addition, few observations were taken at points to the west of the fault. Thus the local geodetic measurements do not extend far enough away from the plate boundary to determine whether the value of 5.5 ± 0.1 cm/yr found by Minster *et al.* (1974) is appropriate.

Bounds can be put on the parameters if assumptions are made about the values of the other unknowns. If the value of τ is assumed to be 5 years, then a statistical bound on H can be obtained by setting $V_0 = 0$ and finding the lowest value of H such that the rms residual is one standard deviation. If aseismic slip or plate motion is included, not as much viscoelastic relaxation is required to explain the data, leading to a larger estimate of H. Model 14B is the resulting bound: $H \approx 10.5$ km.

With respect to τ, the inversions show that the data can be characterized by time constants of from 5 to 1000 years. The latter value implies that viscoelasticity plays virtually no role in the angle change process. Thus, no upper bound can be placed on τ. Also, no lower bound can be found for τ because any such value depends strongly upon the value assumed for H. For example, the surface displacements for a model in which H is given and τ is set equal to 1000 years are about the same as those for a model in which $\tau = 0$ and H is greater than 100 km.

Reasonable bounds on V_0 can be taken as 0 and -2.75 cm/yr, the latter value being that obtained from Minster *et al.* (1974). An upper bound cannot be placed on y_0 since models with $V_0 = 0$ can be found which fit the data (14B) and in such a case the value of y_0 is arbitrary. For $V_0 = -2.75$ cm/yr, a lower bound on y_0 can be obtained by not allowing aseismic slip or viscoelastic relaxation. Thus we inverted the data with V_0 fixed at -2.75 cm/yr and with a starting model in which $\tau = 1000$ yr. The resulting bound, 35 km, is illustrated by model 12B.

The Point Arena measurements were analysed in the same way as the Bay area data. Of the 'thick' elastic layer models with starting values of H equal to 50 km, the following fit the data to within two standard deviations:

(i) Aseismic slip and gross plate motion; (ii) Viscoelasticity and steady plate motion; (iii) Aseismic slip, viscoelasticity, and steady state plate motion.

Among the 'thin' layer models, the following fit the data, again to within two standard deviations:

(i) Aseismic slip and steady state plate motion; (ii) Viscoelasticity and steady relative plate motion; (iii) Aseismic slip, viscoelasticity, and steady state plate motion; (iv) Viscoelasticity alone.

As in the Bay area, gross plate motion alone can fit the data.

A model with V_0 equal to the value found by Minster *et al.* (1974) can again be found: 11P (the P denotes Point Arena models). As in the Bay area, y_0 is again hundreds of kilometres in magnitude for $V_0 = -2.75$ cm/yr. This result provides additional support for a large distance scale for the plate driving force.

A lower limit can be placed on the layer thickness H by assuming $\tau = 5$ yr, by requiring $V_0 = 0$ cm/yr, and then inverting for H. Model 13P is the result: $H \approx 17.0$ km. Note however that model 11P illustrates that values of H smaller than 17.0 are consistent with the data if τ is greater than 5 yr.

Table 2. Results of inversions with models allowing viscoelastic relaxation, gross relative plate motion, steady state slip and episodic slip. t_1 is the time of onset of episodic slip, t_2 is the time at which episodic slip ends and V_{ep} is the constant relative episodic slip velocity (equation (4)).

Model No.	H (km)	τ (yr)	y_0 (km)	V_0 (cm/yr)	t_1 (yr)	t_2 (yr)	V_{ep} (cm/yr)
San Francisco Bay							
1	50.0	1000.0	19.8	−1.47	−10.0	15.0	+4.0
2	20	10.0	50.0	−1.0	−10.0	30.0	−2.0
Point Arena							
1	18.0	9.94	299.9	−1.9	−10.0	25.0	−2.0

As discussed in connection with the Bay area data, τ cannot be bounded. V_0 must again lie between 0 and −2.75 cm/yr, and the latter value can be used in the manner described previously to yield a lower limit on y_0 of 80.0 km (model 14P).

4.2 MODELS WITH EPISODIC SLIP

The results of several inversions with models allowing viscoelastic relaxation, steady aseismic slip, episodic aseismic slip and gross relative plate motion are given in Table 2. In these inversions, t_1 (the onset time of slip), t_2 (the time at which slip ended) and V_{ep} (the relative slip velocity) were held constant while H, τ, y_0 and V_0 were allowed to vary. Our purpose was to show that reasonable values of t_1, t_2 and V_{ep} can be used in models which fit the data. No improvement was expected in the degree of model uniqueness by allowing t_1, t_2 and V_{ep} to vary. Interestingly, the data can be fit even with the left lateral episodic slip as the positive value for V_{ep} in model 1B of Table 2 shows.

5 Discussion

Nur & Mavko (1974) found that a thrust dislocation in an elastic layer over a linear viscoelastic half-space could explain the changes in elevation observed following the 1974 Nankaido earthquake. They also found that the half-space relaxation process can be characterized by time constants τ of about 3–5 yr. Due to the difference in properties assigned to the half-space between the Nur & Mavko (1974) work and ours, a result $\tau = 5$ yr corresponds in the former case to an effective viscosity of 5×10^{19} P and in our case to 1.3×10^{20} P, assuming an average rigidity (Nur & Mavko 1974) for the elastic layer of 8×10^{11} dynes/cm^2.

An important consequence of including viscoelasticity in a fault model is that it provides a means for inducing partial stress recovery following the earthquake. Faulting releases stress in the upper elastic region and stresses the lower viscoelastic regime, which had remained stress-free by virtue of its ability to flow under the slowly applied forces that led to the fracture. Following the rupture, the viscoelastic zone relaxes, transferring its stress to the elastic layer. Although all of the elastic layer is to some degree restressed, the effect is greatest around the ends of the fault, where the coseismic dislocation function changes rapidly. The stress, which had been high in this region following the earthquake (although perhaps not high enough to cause further rupturing) becomes higher still. These sites, where the dislocation function changes rapidly, are prime candidates for shocks following the main event.

The restressing of the elastic layer also reduces the waiting time until the next large shock. Instead of having to regenerate all the strain lost in the main event, relative plate motion need only supply the difference between the strain lost and regained in the half-space relaxation process. The amount of strain regained will depend upon the thickness of the lithosphere, the depth of faulting, and the elastic and viscoelastic properties of the layer and the asthenosphere. In an extreme case, where an earthquake breaks completely through a relatively thin elastic layer (Rundle & Jackson 1977b), the surface shear stress recovery in the neighbourhood of the fault is ~ 80 per cent. For a viscoelastic model of the 1906 San Francisco event whose elastic layer thickness is ~ 20 km, the surface stress recovery is ~ 20 per cent, and for a model whose elastic layer thickness is ~ 50 km, the stress recovery is ~ 5 per cent.

Several authors, for example Brune (1974), have argued that if the lithosphere in California were thin, earthquakes rupturing its entire thickness would produce coseismic deformations extending out from the fault to a distance approximately equal to the fault length. This argument presupposes a model consisting of an elastic layer overlying a viscous region whose rigidity is small. As shown here, however, a model which responds by viscoelastic flow to forces applied over long times can also behave as an elastic half-space over a short period of time following brittle fracture. The coseismic displacements for such a model extend out from the fault a distance of the order of its depth. The thickness of the lithosphere in relation to the depth of fracture is important only for the post-seismic displacements (Rundle & Jackson 1977b).

Viscoelastic relaxation is an attractive candidate for explaining not only the geodetic data but also the stress recovery phenomenon thought to occur after large earthquakes. However, the inversion process can yield no firm determination of the model parameters associated with the post-seismic angle changes. Models which include many different combinations of viscoelasticity, aseismic slip below a 10-km seismic zone and a steady plate motion are able to fit the data in both the Bay area and Point Arena. This model nonuniqueness raises two questions:

(i) Given data errors of ~ 2 arcsec, how many data are needed to unambiguously solve for the model parameters?

(ii) Using roughly ~ 30–40 observations, how accurately do the survey measurements have to be made in order to find a unique model?

To answer question (i), we generated 500 synthetic angle changes for a specific choice of elastic layer thickness H, time constant τ, distance scale y_0 and velocity V_0. A random number generated from a distribution with mean zero and standard deviation 2 arcsec was added to each angle change. First 50, then 150 and finally 500 artificial data points were inverted to find whether a larger number of data would allow a unique determination of the model parameters. We found that convergence to a unique model was not satisfactory in any case.

Alternatively, we can determine how many observations are needed to afford a unique, minimum variance model if the errors in the data have variance σ_y^2. As derived in the Appendix, an estimate of the variance of a standardized model parameter is

$$\sigma_x^2 \approx 1 - \frac{p}{4} + \frac{\sigma_y^2}{4} \sum_{i=1}^{p} \frac{1}{\lambda_i^2} \tag{5}$$

where p is the number of eigenvalues used in constructing the inverse. For each value of p, (5) defines σ_x^2 as a linear function of σ_y^2 (see Fig. 5). Table 3 gives the σ_x^2 intercept and the slope of the line shown in Fig. 5 for the Point Arena data and the reference model $H = 20$ km,

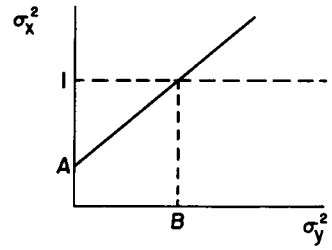

Figure 5. Dependence of the model parameter variance σ_x^2 upon the variance in the data σ_y^2. The intercept of the line is indicated by A, and the value of σ_y^2 corresponding to $\sigma_x^2 = 1$ is indicated by B (see Table 3).

Table 3. Dependence of the model parameter variance σ_x^2 upon the variance in the data σ_y^2 for the number of nonzero eigenvalues p varying from 1 to 4. Column 1 gives p, column 2 gives the σ_x^2 intercept A and column 3 gives the slope of the σ_x^2 versus σ_y^2 line (see Fig. 5). Column 4 gives the value B of σ_y^2 corresponding to $\sigma_x^2 = 1$ and column 5 gives the square root of B.

p	A	Slope	B	$\sqrt{B}$
1	0.75	4.1×10^{-2}	605.2	24.6
2	0.50	3.53	1.4×10^{-3}	0.4
3	0.25	81.61	9.2×10^{-3}	9.6×10^{-2}
4	0	21267.78	4.8×10^{-5}	6.9×10^{-3}

$\tau = 5.1$ yr, $y_0 = 21.0$ km and $V_0 = -0.08$ cm/yr. The standard deviations used to standardize the model parameters according to (A4), $\omega_H = 6$ km, $\omega_\tau = 4$ yr, $\omega_{y_0} = 10$ km and $\omega_{V_0} = 2$ cm/yr, were determined both on physical grounds and by the requirement that the inversion iteration converge. Both slope and intercept of the $\sigma_x^2 - \sigma_y^2$ line are shown in Table 3 for $p = 1$ to 4. Since the parameters have been standardized, the maximum value of σ_y^2 allowing a uniquely determined model can be estimated by putting $\sigma_x^2 = 0.25$ and setting $p = 4$. This procedure is roughly equivalent to requiring that the standard deviation of each model parameter be one-half its *a priori* value. The resulting maximum observational error is 1.7×10^{-3} arcsec. As discussed in connection with the model assumptions, layers of anomalous rigidity either at depth or near the surface probably contribute spurious angle changes of the order of an arc second, so the reduction of σ_y to 1.7×10^{-3} s by improved observing techniques is probably impossible.

From Table 3 it can also be seen why increasing the number of synthetic data from 50 to 500 in (i) had little effect on the convergence of the iteration. The variance of the sum of N independent random variables with mean 0 and individual variance 1 is N. To require that the model parameters in the case $p = 4$ be known to within roughly half their *a priori* standard deviations ($\sigma_x = \frac{1}{2}$) while allowing the data error σ_y to remain at 2 arcsec would therefore require the number of observations N to be

$$N > 4/(1.2 \times 10^{-5}) \sim 3.2 \times 10^5. \tag{6}$$

In the light of (6), the difference in (i) between 50 and 500 observations is negligible.

Another way of illustrating the model nonuniqueness is with the use of a residual map. Let us define the root mean square residual ϵ between the observed data y_i and 'theoretical' data y_i^* by

$$\epsilon = \sqrt{\left[\left[\sum_{i=1}^{n} [(y_i - y_i^*)^2/\sigma_y^2]\right]\right]} \tag{7}$$

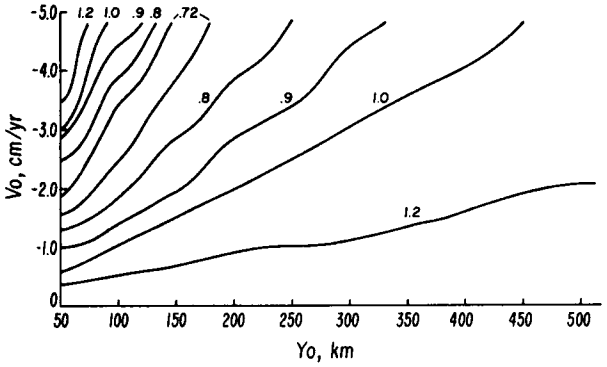

Figure 6. Residual map for Bay area data. H and τ are fixed at 10.1 km and 993.3 yr respectively.

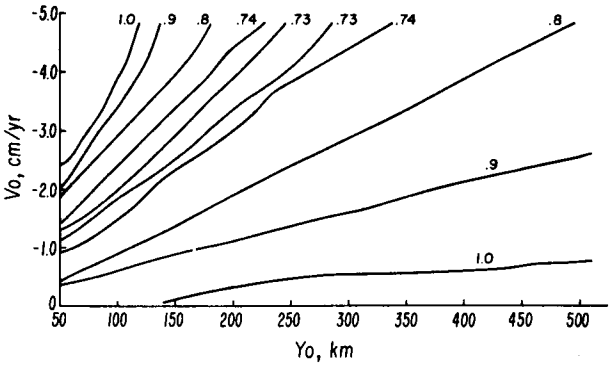

Figure 7. Residual map for Bay area data. H and τ are fixed at 20.0 km and 5.0 yr respectively.

Since the data have been standardized through division by σ_y a criterion useful in determining the fit of the model is that ϵ be small (Jackson 1972).

If two of the parameters H, τ, y_0 and V_0 are fixed at some value, we can construct a residual map by allowing the two free parameters to vary and plotting contours of equal ϵ. Figs 6 and 7 illustrate this technique, with V_0 and y_0 the two free parameters. In Fig. 6, $H = 10.1$ km, $\tau = 993.3$ yr, and in Fig. 7, $H = 20.0$ km, $\tau = 5.0$ yr. Aseismic slip was not allowed in either case. It is clear that there are many models which meet the criterion that ϵ be less than 1. It can also be seen that for models without viscoelasticity (Fig. 6), the least squares value of y_0 is smaller for a given V_0 than it is for models with viscoelasticity (Fig. 7). Although a lower bound on y_0 of 35 km was obtained earlier, it was based on the requirement that $\epsilon \leqslant 1$. If instead we demand that ϵ be a minimum, $y_0 \approx 100$ km with $V_0 = -2.75$ cm/yr.

The fact that the data can be fit by our viscoelastic model appears to contradict the usual assumption that most of the plate deformation is concentrated within 10 km of the fault. For example, two points each situated 100 km from the fault on opposite sides would show a relative displacement of 1.1 m for the best-fitting model without viscoelastic relaxation or aseismic slip, and with $V_0 = -2.75$ cm/yr and $y_0 = 100$ km. As another example, Rundle & Jackson (1977b) show a viscoelastic model in which a long fault breaks completely through a 20-km thick elastic layer. Even at 100 km away from the fault, the *post-seismic* deformation is one quarter of the *coseismic* deformation at the fault trace.

Wayne Thatcher (private communication) has recently brought to our attention the fact that the relative displacement of Farallon with respect to Mt Diablo was less than ~ 1.5 m during the years 1906–1947. Although this information was received after the work

reported here was completed, it can easily be verified using Figs 6 and 7 that it too is consistent with the model we describe.

An argument often used to support the contention that post-seismic deformation is concentrated within 10 km of the San Andreas is that the shear straining is highest near the fault and drops to a very low value somewhat farther away. The pattern of shear straining generated by the model we describe is very similar. From Rundle & Jackson (1977) it can be seen that most of the rapid change in viscoelastic displacements occurs close to the fault, producing the highest shear strains. The slow decay with distance of the displacements beyond ~ 30 km produces only a very low amount of shear straining.

Conclusions

We have attempted to develop a realistic model of large strike slip earthquakes. Since faulting on the scale of the 1906 San Francisco event involves a large portion of the Earth's crust, and releases large amounts of both stress and energy, it is reasonable to suppose that the Earth's viscous as well as elastic properties play a significant role. It is known that the region at the base of the lithosphere represents a relatively non-rigid zone over which the more elastic surface layer can move. It is conceivable that zones or pockets of such relatively non-rigid material may extend to shallower depths, particularly beneath highly stressed or sheared areas of the lithosphere such as the San Andreas fault zone. In order to investigate these possibilities, we required that our model include gross relative plate motion, viscoelastic relaxation, and aseismic slip at depth.

Our most important conclusion is that viscoelastic relaxation can explain the post-seismic movements frequently observed following large crustal strike slip earthquakes. Models with either a thick or thin elastic layer overlying a viscoelastic half-space were found which fit the observations as well as purely elastic models. As the viscoelastic model incorporates many of the mechanisms thought to be operating at depth on the San Andreas, and for example can logically explain the stress recovery phenomenon, we believe it to be a realistic description of the San Andreas fault.

A second significant conclusion is that the horizontal distance scale for the plate driving forces is probably greater than 100 km, assuming that the gross relative plate motion is the value given by Minster *et al.* (1974), 5.5 cm/yr. If the plates are driven by fluid motions, the result $y_0 \gtrsim 100$ km implies that the low viscosity zone which the fluid flow occupies is at least 100 km thick, since on physical grounds the horizontal and vertical characteristic distance scales must be similar. For other possible plate driving forces the physical meaning of $y_0 \gtrsim 100$ km is not clear.

Finally, it was found that with the geodetic triangulation techniques used previous to ~ 1950, a unique determination of the model parameters to within acceptably small standard deviations is impossible if the number of data is less than 3.2×10^5.

Acknowledgment

We would like to thank Dr Wayne Thatcher of the USGS for helpful comments and discussions.

References

Brace, W. & Byerlee, J., 1966. Stick-slip as a mechanism for earthquakes, *Science*, **153**, 990.

Brace, W. & Byerlee, J., 1970. California earthquakes: Why only shallow focus?, *Science*, **168**, 1573.

Brune, J., 1974. Current status of understanding quasi-permanent fields associated with earthquakes, *Trans. Am. geophys. Un. EOS*, **55**, 820.

Byerlee, J. & Brace, W., 1968. Stick-slip, stable sliding and earthquakes – effect of rock type, pressure, strain rate and stiffness, *J. geophys. Res.*, **73**, 6031.

Chinnery, M., 1961. The deformation of the ground around surface faults, *Bull. seism. Soc. Am.*, **51**, 355.

Chinnery, M., 1963. The stress changes that accompany strike-slip faulting, *Bull. seism. Soc. Am.*, **53**, 921.

Crittenden, M., 1963. Effective viscosity of the earth derived from isostatic loading of plesitocene Lake Bonneville, *J. geophys. Res.*, **68**, 5517.

Crough, S., 1975. Thermal model of oceanic lithosphere, *Nature*, **256**, 388.

Forsyth, D. & Uyeda, S., 1975. On the relative importance of the driving forces of plate motion, *Geophys. J. R. astr. Soc.*, **43**, 163.

Hobbs, B. E., McLaren, A. C. & Paterson, M. S., 1972. Plasticity of single crystals of synthetic quartz, *Flow and fracture of rocks*, p. 16, eds H. C. Heard, I. Y. Borg, N. L. Carter and C. B. Raleigh, Am. geophys. Un.

Isacks, B., Oliver, J. & Sykes, L., 1968. Seismology and the new global tectonics, *J. geophys. Res.*, **73**, 5855.

Jackson, D., 1971a. The attenuation of Love waves and toroidal oscillations of the earth, *Geophys. J. R. astr. Soc.*, **25**, 25.

Jackson, D., 1971b. Attenuation of seismic waves by grain boundary relaxation, *Proc. nat. Acad. Sci.*, **68**, 1577.

Jackson, D., 1972. Interpretation of inaccurate, insufficient and inconsistent data, *Geophys. J. R. astr. Soc.*, **29**, 97.

Jackson, D., 1973. Marginal solutions to quasi-linear inverse problems in geophysics: The edgehog method, *Geophys. J. R. astr. Soc.*, **35**, 121.

Jackson, D., 1974. *Tradeoffs and simultaneous optimizations in inverse problems*, unpublished manuscript.

Lachenbruch, A. & Sass, J., 1973. Thermo-mechanical aspects of the fault zone, in *Proc. Conf. Tectonic Problems San Andreas Fault System*, eds A. Nur & R. Kovach, Stanford University Publications in the Geological Sciences 13.

Leeds, A., 1975. Lithospheric thickness in the Western Pacific, *Phys. Earth planet. Int.*, **11**, 61.

Maruyama, T., 1964. Statistical elastic dislocations in an infinite and semi-infinite medium, *Tokyo Univ. Earthquake Res. Inst. Bull.*, **42**, 289.

Mavko, G. & Nur, A., 1975. Melt squirt in the asthenosphere, *J. geophys. Res.*, **80**, 1444.

McConnell, R., 1965. Isostatic adjustment in a layered earth, *J. geophys. Res.*, **70**, 5171.

Meade, B. (ed), 1973. Reports on geodetic measurements of crustal movement, 1906–71, *USGPO Publ. No. 0317-00167*, Rockville, Maryland.

Minster, J., Jordan, T., Molnar, P. & Haynes, E., 1974. Numerical modelling of instantaneous plate tectonics, *Geophys. J. R. astr. Soc.*, **36**, 541.

Nur, A. & Mavko, G., 1974. Postseismic viscoelastic rebound, *Science*, **183**, 204.

Peltier, W. R., 1974. The impulse response of a Maxwell earth, *Rev. Geophys. Space Phys.*, **12**, 649.

Press, F., 1965. Displacement, strains and tilts at teleseismic distances, *J. geophys. Res.*, **70**, 2395.

Rundle, J. B., 1976. Anelastic processes in strike-slip faulting: application to the San Francisco Earthquake of 1906, *PhD dissertation*, UCLA.

Rundle, J. B. & Jackson, D. D., 1977a. *Pure appl. Geophys.*, in press.

Rundle, J. B. & Jackson, D. D., 1977b. A three-dimensional viscoelastic model of a strike slip fault. *Geophys. J. R. astr. Soc.*, **49**, 575.

Savage, J. & Burford, R., 1973. Geodetic determination of relative plate motion in central California, *J. geophys. Res.*, **78**, 832.

Sclater, J. & Francheteau, J., 1970. The implications of terrestrial heat flow observations on current tectonic and geochemical models of the crust and upper mantle of the earth, *Geophys. J. R. astr. Soc.*, **20**, 509.

Steketee, J., 1958. On Volterra's dislocations in a semi-infinite elastic medium, *Can. J. Phys.*, **36**, 192.

Thatcher, W., 1974. Strain release mechanism of the 1906 San Francisco earthquake, *Science*, **184**, 1283.

Thatcher, W., 1975a. Strain accumulation and release mechanism of the 1906 San Francisco earthquake, *J. geophys. Res.*, **80**, 4862.

Thatcher, W., 1975b. Strain accumulation on the northern San Andreas fault zone since 1906, *J. geophys. Res.*, **80**, 4873.

Turcotte, D. & Spence, D., 1974. An analysis of strain accumulation on a strike slip fault, *J. geophys. Res.*, 79, 4407.

Appendix

If we have n statistically independent data $\mathbf{y} = (y_1, y_2, \ldots, y_n)$ and m linearly related model parameters $\mathbf{x} = (x_1, x_2, \ldots, x_m)$, we can in general write the forward problem as

$$\mathbf{y} = \mathbf{A}\mathbf{x} \tag{A1}$$

where $\mathbf{A}$ is a known matrix. We next write the $m \times m$ matrix product $\mathbf{A}^T\mathbf{A}$, where the superscript T denotes the transpose operation. Assuming $\mathbf{A}^T\mathbf{A}$, has rank m we define the $m \times m$ matrices Λ and $\mathbf{V}$ as

$$\Lambda \equiv \begin{bmatrix} \lambda_1 & & & \\ & \lambda_2 & & 0 \\ & & \ddots & \\ 0 & & & \lambda_m \end{bmatrix}$$

$$\mathbf{V} \equiv (\mathbf{v}^1 \mathbf{v}^2 \ldots \mathbf{v}^m) \tag{A2}$$

λ_1 is the largest eigenvalue of $\mathbf{A}^T\mathbf{A}$ with associated column eigenvector $\mathbf{v}^1$, λ_2 is the next largest eigenvalue of $\mathbf{A}^T\mathbf{A}$ with column eigenvector $\mathbf{v}^2$ and so on.

If $\mathbf{A}^T\mathbf{A}$ is of rank $p < m$ or if $m - p$ of the eigenvalues are so small in relation to λ_1 that they provide no useful information, we can define a new $m \times m$ matrix Λ^p from Λ:

$$\Lambda^p = \begin{bmatrix} \lambda_1 & & & & & & \\ & \lambda_2 & & & & & \\ & & \ddots & & & & \\ & & & \lambda_p & & 0 & \\ 0 & & & & 0 & & \\ & & & & & \ddots & \\ & & & & & & 0 \end{bmatrix} = \Lambda \mathbf{I}^p \tag{A3}$$

where the $\mathbf{I}^p$ is the $m \times m$ matrix of zeroes except for the first p diagonal elements, which are 1.

The x_i can be considered to be random variables since they are linearly related to the independent data y_i. Thus we can 'standardize' the model parameters by dividing them by a set of assumed *a priori* errors ω

$$x_i' = \frac{x_i}{\omega_i}. \tag{A4}$$

We can also define the *a priori* $m \times m$ covariance matrix $\mathbf{C}(x)$ if we assume that the x_i are statistically independent

$$\mathbf{C}(x) = \begin{bmatrix} \omega_1^2 & & & \\ & \omega_2^2 & & 0 \\ & & \ddots & \\ 0 & & & \omega_m^2 \end{bmatrix} \tag{A5}$$

Clearly $C(x') = \mathbf{I}m$ where $\mathbf{I}m$ is the $m \times m$ unit matrix.

Let us now assume that the variables $\mathbf{x}$ have been standardized according to (A4) and that we have obtained a solution $\mathbf{x}^*$ to equation (A1) as in Jackson (1972). If we have used only

p of the eigenvectors in constructing the solution $\mathbf{x}^*$, the new model covariance matrix is (Rundle 1976)

$$\mathbf{C}(x^*) = \mathbf{V}(\mathbf{I}m - \mathbf{I}^p)\,\mathbf{V}^T + \sigma_y^2 \mathbf{V}(\Lambda^p)^{-2}\mathbf{V}^T \tag{A6}$$

where σ_y is the standard deviation of the data errors.

As an indication of how the standard deviations of the standardized model parameters depend on σ_y, let us take the trace of (A6), which represents the sum of the variances of the parameters

$$Tr\mathbf{C}(x^*) = 4 - p + \sigma_y^2 \sum_{i=1}^{p} \frac{1}{\lambda_i^2} \tag{A7}$$

where p is the number of nonzero eigenvalues. Clearly, small eigenvalues produce a large uncertainty in the model parameters. If $p = 0$, the data provide no information and $\sigma_x^2 = 1$. The data are only useful if $\sigma_x^2 < 1$. Assuming $p \equiv 4$, we have a unique solution and the variance can be estimated by

$$\sigma_x^2 \sim \tfrac{1}{4}Tr(\mathbf{C}(x^*)) = \frac{\sigma_y^2}{4} \sum_{i=1}^{4} \frac{1}{\lambda_1^2}, \tag{A8}$$

If in the model fitting process some of the small eigenvalues have been set equal to zero to decrease the uncertainty in the unknowns, $p < 4$, and an estimate of the variance is

$$\sigma_x^2 \approx 1 - \frac{p}{4} + \frac{\sigma_y^2}{4} \sum_{i=1}^{p} \frac{1}{\lambda_i^2}\,. \tag{A9}$$